EPJ Web of Conferences **114**, 02010 (2016)
DOI: 10.1051/epjconf/201611402010


# The effect of porosity on performance of phosphoric acid doped polybenzimidazole polymer electrolyte membrane fuel cell

Muhammet Celik[1], Gamze Genc[2,a], Gulsah Elden[2] and Huseyin Yapici[2]

[1]*Aksaray University, Dept. of Mechanical Engineering, 68100, Aksaray, Turkey*
[2]*Erciyes University, Dept. of Energy Systems Engineering, 38039, Kayseri, Turkey*

**Abstract.** A polybenzimidazole (PBI) based polymer electrolyte fuel cells, which called high temperature polymer electrolyte fuel cells (HT-PEMS), operate at higher temperatures (120-200°C) than conventional PEM fuel cells. Although it is known that HT-PEMS have some of the significant advantages as non-humidification requirements for membrane and the lack of liquid water at high temperature in the fuel cell, the generated water as a result of oxygen reduction reaction causes in the degradation of these systems. The generated water absorbed into membrane side interacts with the hydrophilic PBI matrix and it can cause swelling of membrane, so water transport mechanism in a membrane electrode assembly (MEA) needs to be well understood and water balance must be calculated in MEA. Therefore, the water diffusion transport across the electrolyte should be determined. In this study, various porosity values of gas diffusion layers are considered in order to investigate the effects of porosity on the water management for two phase flow in fuel cell. Two-dimensional fuel cell with interdigitated flow-field is modelled using COMSOL Multiphysics 4.2a software. The operating temperature and doping level is selected as 160°C and 6.75mol H3PO4/PBI, respectively.

## 1 Introduction

The proton exchange membrane (PEM) fuel cells are the most attractive alternative energy devices that can produce zero-emission power due to the fact that they do not emit harmful products after the electrochemical reactions. Nafion based PEM fuel cells operate under 100°C. But the operation conditions of these fuel cells have some disadvantages such as necessity humidifying membrane, water management problems etc. But Polybenzimidazole (PBI) based PEM fuel cells can solve many of these disadvantages by increasing the operation temperatures above 120°C. By running the PBI PEM fuel cells at 120°C-180°C, the water management becomes easier because the produced water will be in the gas phase.

PBI is an amorphous polymer which has strong thermochemical stability, and proton conductivity can be enhanced by phosphoric acid doping procedure. Because of this advantages, HT-PEMs have been attracted attentions and many studies such as its performance [1-5], CO contamination [6-8], numerical modelling [9-11] have been done. But in the literature the two phase flow in HT-PEMs are very scarce. Especially, the two phase flow at stop conditions should be investigated. Because when the operation of fuel cell finish, the water vapor will be condensed. So, the condensed water will accumulate in the porous structure. The phosphoric acid removal occurs in the presence of liquid water in the porous structure resulting low ionic conductivity of the PBI membrane. With this consideration the condensed water should be lessened inside the fuel cell. In this study the two phase flow at the stop conditions in a PBI based PEM fuel cell is investigated in order to observe how distribution of water change with the porosity of the cathode gas diffusion layer.

## 2 Mathematical Model

Because the water is produced at cathode, the cathode side of the fuel cell is selected as computational domain. The multiphase mixture ($M^2$) approach is used for modelling. The assumptions in numerical model are as follows;

- Gas phase is perfectly a mixture and ideal gas
- Hydrogen and oxygen is soluble in water
- Time-dependent regime

In addition, the fuel cell is in stop conditions when the fuel cell is not running and the electrochemical reactions are stopped. Hence, there is no hydrogen or oxygen entry to the fuel cell.

### 2.1 Governing equations

Mass conservation equation can be given as;

[a] Corresponding author: gamzegenc@erciyes.edu.tr

$$\varepsilon\frac{\partial \rho}{\partial t}+\nabla(\varepsilon\rho u)=0 \quad (1)$$

where $\varepsilon$ is porosity of the gas diffusion layer, $u$ is velocity and $\rho$ is the mixture density. In Eq(1) the $\rho u$ is defined the mixture velocity which can be expressed as;

$$\rho u=\rho_l u_l+\rho_g u_g \quad (2)$$

where $\rho_l$ is the density of the liquid phase, $\rho_g$ is the density of vapor phase, $u_l$ is the liquid phase velocity and $u_g$ is the vapor phase velocity.

The momentum conservation equation for two phase flow can be written as [12];

$$\frac{\partial(\varepsilon\rho u)}{\partial t}+\nabla(\varepsilon\rho uu)=\nabla(\varepsilon\mu\nabla u)-\varepsilon\nabla p+\varepsilon\rho_k g-\varepsilon^2\frac{\mu}{K}u \quad (3)$$

where the first term in the left hand side defines the variation of the momentum according to time. Second term defines the momentum according to convection. At the right hand side the variation of the momentum by viscous forces, pressure gradients, and gravity can be seen. The last term in the right hand side defines the flow in the porous structure. k subscript describes the phases (liquid and gas phase).

The viscosity of the two phase mixture can be expressed as [12];

$$\mu=\frac{\rho_l s+\rho_g(1-s)}{(k_{rl}/\nu_l)+(k_{rg}/\nu_g)} \quad (4)$$

where $k_{rl}$ and $k_{rg}$ describes relative permeability for liquid phase and gas phase, respectively. s defines the saturation of water. Relative permeabilities according the saturation can be defined as;

$$k_{rl}=s^3 \quad (5)$$

$$k_{rg}=(1-s)^3 \quad (6)$$

The saturation of water can be written as [13];

$$s=\frac{C^{H_2O}-C_g^{H_2O}}{C_l-C_g^{H_2O}} \quad (7)$$

where $C_{H2O}$ is the mixture concentration, $C_g^{H2O}$ is gas phase concentration and $C_l$ is liquid concentration.

The species equation can be expressed as [14];

$$\varepsilon\frac{\partial C^{H_2O}}{\partial t}+\nabla\cdot(\varepsilon\gamma_c\vec{u}C^{H_2O})=\nabla\cdot(D_g^{H_2O}\nabla C_g^{H_2O})-\nabla\cdot\left[\left(\frac{mf_l^{H_2O}}{M^{H_2O}}-\frac{C_g^{H_2O}}{\rho_g}\right)\vec{j}_l\right] \quad (8)$$

where $\gamma_c$ defines advection correction factor, $\vec{j}_l$ is diffusion flux and $mf_l^{H_2O}$ describes the mass fraction of liquid water. While the first term at the right hand side defines the diffusion of gas phase, the second term defines the motion according to capillary effect. The advection correction factor for water can be expressed as [12];

$$\gamma_{H_2O}=\frac{\rho(\lambda_l C_l^{H_2O}+\lambda_g C_g^{H_2O})}{\rho_l s C_l^{H_2O}+\rho_g(1-s)C_g^{H_2O}} \quad (9)$$

where $\lambda_l$ and $\lambda_g$ are the relative mobility for the liquid phase and gas phase, respectively. Relative mobilities can be defined as [12];

$$\lambda_l(s)=\frac{k_{rl}/\nu_l}{k_{rl}/\nu_l+k_{rg}/\nu_g} \quad (10)$$

$$\lambda_g(s)=1-\lambda_l(s) \quad (11)$$

Diffusion flux, $\vec{j}_l$, can be expressed as [13];

$$j_l=\frac{\lambda_l\lambda_g K}{\nu}\nabla P_c \quad (12)$$

Capillary pressure, $P_c$, can be expressed according to hydrophilic and hydrophobic surfaces. In this study the gas diffusion layer has hydrophobic structure. Hence, the capillary pressure for hydrophobic structure can be written as [13];

$$P_c=\sigma\cos\theta_c\left(\frac{\varepsilon}{K}\right)^{\frac{1}{2}}\left[1.417s-2.120s^2+1.263s^3\right] \quad (13)$$

where $\sigma$ describes the surface tension, $\theta_c$ describes the contact angle.

## 2.2 Numerical Procedure

In the numerical solutions, *COMSOL Multiphysics 4.2a* software which is based a finite element method solver is used. The computational domain and grid structure can be seen in Figure 1.

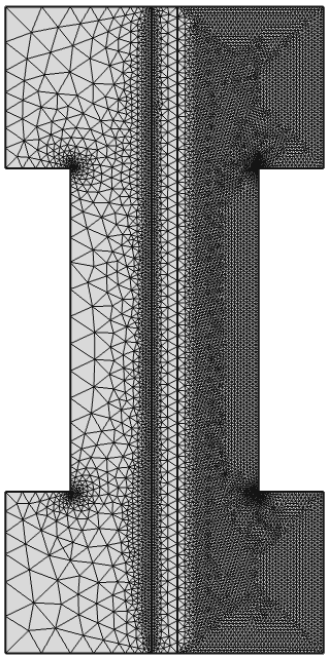

**Figure 1.** Computational domain and grid structure

As can be seen in Table 1, the parametric variations are observed according to numerical solutions for different element numbers. It is assumed that the

parameter values are the same for 18522 and higher element numbers. So, the element number for the numerical model is chosen as 18522. Grid structure consists of 18522 triangular elements and the solver is selected as PARDISO. The parameters used in the modeling are listed in Table 2.

**Table 1.** Parametric variations according to element number

| **Element Number** | **12772** | **18522** | **41097** |
|---|---|---|---|
| Saturation | 2.553E-4 | 2.555 E-4 | 2.557 E-4 |
| Temperature[K] | 338.70 | 338.70 | 338.70 |

**Table 2.** Model Parameters.

| **Parameter** | **Value** |
|---|---|
| Surface Tension | 0.0625 N/m [14] |
| GDL porosity | 0.4-0.7 |
| GDL contact angle | 110$^{o}$ [14] |
| Operation pressure | 101325 Pa |
| Initial temperature | 180$^{o}$C |
| Acid doping level | 6.75 mol H3PO4/PBI |

## 3 Results and Discussions

The saturation according to time for GDL porosity of 0.4 is given in Figure 2. As can be seen in this Figure, the saturation increased with time and it became constant after 80 s. It means all of the gas phase condensed to the liquid phase in 100 s.

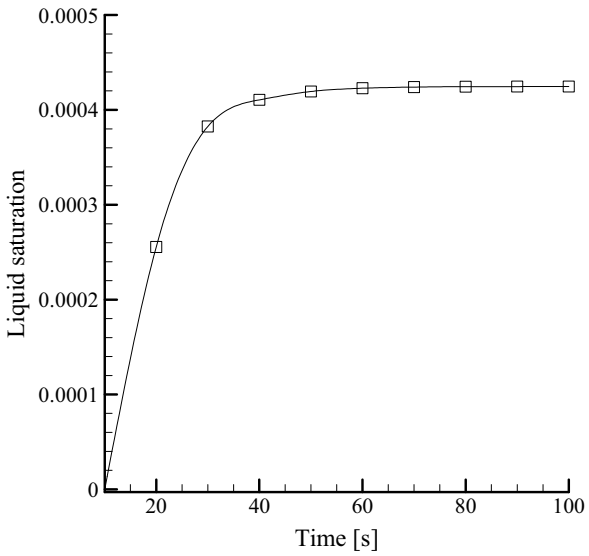


**Figure 2.** Saturation according to time (ε=0.5)

The saturation distribution according to time for GDL porosity of 0.4 is given in Figure 3. The saturation is higher at the centre of the gas diffusion layer due to the fact that the heat transfer from fuel cell to environment occurs at the interface of the gas diffusion layer and gas channel. As is seen in this figure, at the 100s, the saturation distribution became uniform in cathode gas diffusion layer and it means all of the gas phase condensed to liquid phase.

The diffusion of gas phase is relative to porosity of the medium. The gas molecules can effectively diffuse in the porous structure at higher porosity levels. In the Figure 4, the change of saturation according to porosity of the GDL at t=50s is given. While the porosity increases, the saturation level decreases. Because the gas molecules are transported effectively into the porous structure and they leave the cell before condensation, so it decreases the saturation level.

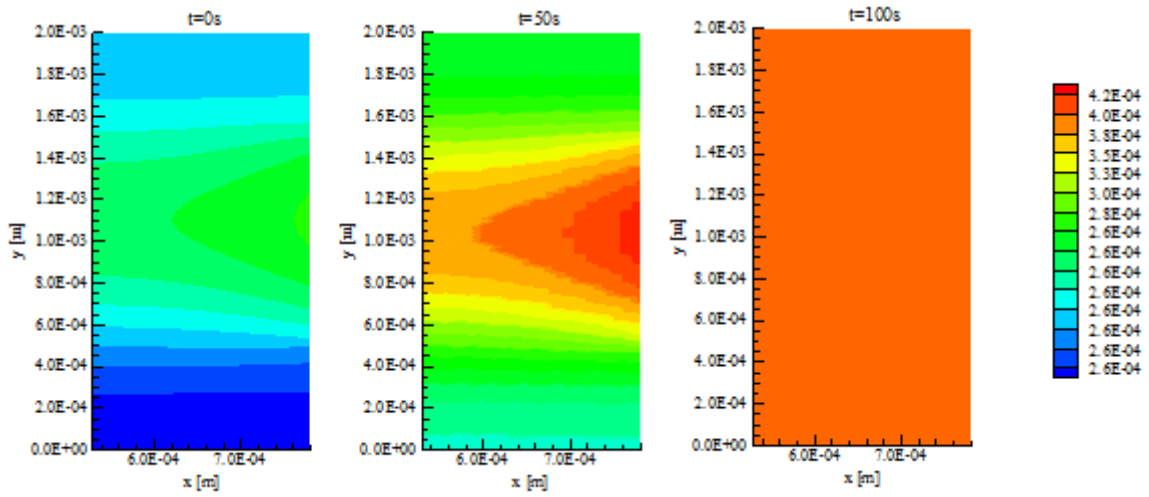


**Figure 3.** Saturation variation according to time (ε=0.5)

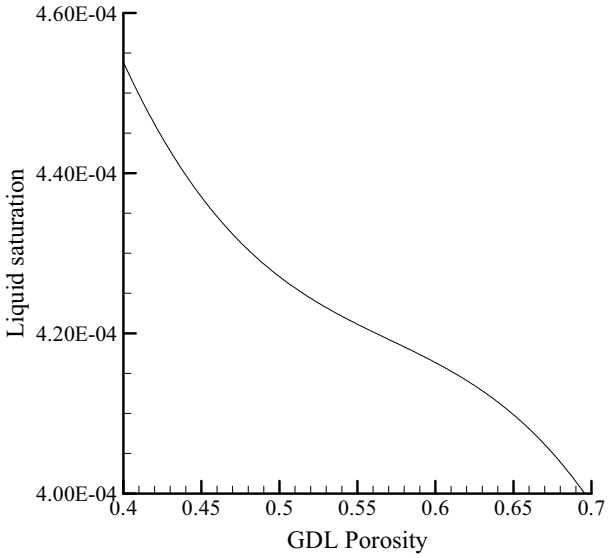


**Figure 4.** Saturation according to GDL porosity (t=50s)

In order to investigate the effect of GDL porosity in detail, a constant saturation level is selected as $4.2 \cdot 10^{-4}$. Time needed to reach saturation level of $4.2 \cdot 10^{-4}$ according to GDL porosity is given in Figure 5. As can be seen from this figure, time needed is increasing with increasing GDL porosity. When GDL porosity is 0.5, 36.2s needed to reach the saturation level of $4.2\ 10^{-4}$. It means while increasing the GDL porosity, the gas phase presence in the medium decreases. Therefore, the lower condensations occur at high GDL porosity.

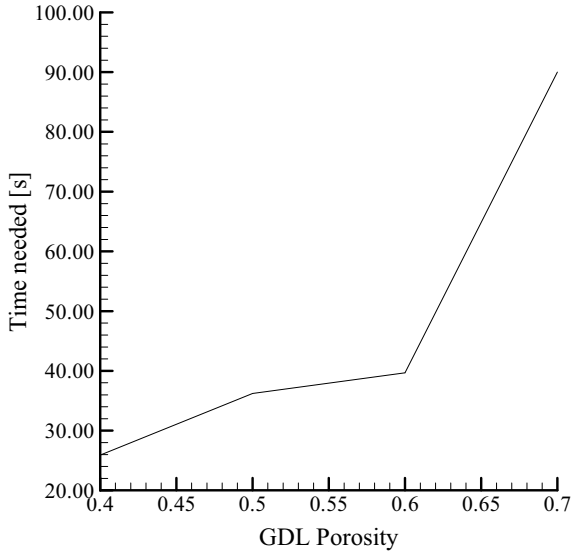


**Figure 5.** Time needed to reach desired saturation level according to GDL porosity

## 4 Conclusions

In this study, a transient, two dimensional, two phase numerical model for PBI based PEM fuel cell was made. Firstly, for the base case (ε=0.5), the saturation variation according to time was discussed. After that, for the various GDL porosity values (ε=0.4-0.7), the saturation level was investigated. Finally, the time needed to reach desired saturation level according to porosity was investigated. According to numerical solutions, it can be said as follows;

- The diffusion of gas molecules are highly related to porosity of gas diffusion layer.
- While porosity of GDL increases the saturation level decreases owing to the fact that the molecules leave the cell before condensation.
- Leaving the gas molecules from the cell facilitate the water management.

## Acknowledgements

The authors would like to thank the Scientific Research Projects Unit of Erciyes University for funding supported by project coded FDK-2014-5442 and Scientific and Technological Research Council of Turkey (TÜBİTAK) for funding supported by project coded 111M071.

## References

1. D.Cheddie, N. Munroe, Energ Convers Manage **47,** 11 (2006)
2. D.F. Cheddie, N.D.H. Munroe, J Power Sources **160,** 1 (2006)
3. J. Hu, H. Zhang, J. Hu, Y. ZhaiB. Yi, J Power Sources **160,** 2 (2006)
4. A. Su, Y. Ferng, J. HouT. Yu, Int J Hydrogen Energ **37,** 9 (2012)
5. R. Taccani, N. Zuliani, , Int J Hydrogen Energ **36,** 16 (2011)
6. S.J. Andreasen, J.R. Vang, S.K. Kær, Int J Hydrogen Energ **36,** 16 (2011)
7. A.R. Korsgaard, M.P. Nielsen, M. BangS.r.K. Kær. *Modeling of CO influence in PBI electrolyte PEM fuel cells*. in *ASME 2006 4th International Conference on Fuel Cell Science, Engineering and Technology*. 2006. American Society of Mechanical Engineers.
8. F. Seland, T. Berning, B. Børresen, R. Tunold, J Power Sources **160,** 1 (2006)
9. K. Jiao, X. Li, Fuel Cells **10,** 3 (2010)
10. C. Siegel, G. Bandlamudi, A. Heinzel, J Power Sources **196,** 5 (2011)
11. T. Sousa, M. Mamlouk, K. Scott, Chem Eng Sci **65,** 8 (2010)
12. Z.H. Wang, C.Y. Wang, K.S. Chen, J Power Sources **94,** 1 (2001)
13. U. Pasaogullari, C.Y. Wang, K.S. Chen, J Electrochem Soc **152,** 8 (2005)
14. U. Pasaogullari, C.Y. Wang, J Electrochem Soc **152,** 2 (2005)